Tripling the capacity of wireless communications using electromagnetic polarization

Michael R. Andrews*, Partha P. Mitra* & Robert deCarvalho*†

* *Bell Labs, Lucent Technologies, Murray Hill, New Jersey 07974, USA*
† *Harvard University, Cambridge, Massachusetts 02138, USA*

Wireless communications are a fundamental part of modern information infrastructure. But wireless bandwidth is costly[1], prompting a close examination of the data channels available using electromagnetic waves. Classically, radio communications have relied on one channel per frequency, although it is well understood that the two polarization states of planar waves[2] allow two distinct information channels; techniques such as 'polarization diversity' already take advantage of this[3]. Recent work[4–7] has shown that environments with scattering, such as urban areas or indoors, also possess independent spatial channels that can be used to enhance capacity greatly. In either case, the relevant signal processing techniques come under the heading of 'multiple-input/multiple-output' communications, because multiple antennae are required to access the polarization or spatial channels. Here we show that, in a scattering environment, an extra factor of three in channel capacity can be obtained, relative to the conventional limit using dual-polarized radio signals. The extra capacity arises because there are six distinguishable electric and magnetic states of polarization at a given point, rather than two as is usually assumed.

In Fig. 1, we show why the presence of a scattering environment violates our intuitive notion of there being only two polarization degrees of freedom for electromagnetic radiation. This situation arises because in free space, radiated electric and magnetic fields are constrained to be perpendicular to one another and to the direction of propagation[2]. Thus, once the direction of propagation is fixed, only two degrees of freedom remain which are typically referred to as either horizontal or vertical (linear) polarizations. In the presence of a reflecting surface, however, multiple paths are possible between the two points. Although the wave propagating along the direct path cannot have an electric field component parallel to that path, the wave propagating along the reflected path can contribute such a component to the field at the receiver (it is effectively a longitudinal component when referred to the line-of-sight). Thus, by using appropriate transmit antennae we can propagate waves which cause independent fluctuations in all three electric field components. The electromagnetic polarization is no longer constrained to be perpendicular to the line-of-sight[8]. The presence of a single reflecting surface allows the use of three channels of electric-field polarization for wireless communication.

In order to make our statements more precise, we introduce H, a 6×6 matrix relating the electric ($\mathbf{E}$) and magnetic ($\mathbf{B}$) fields measured at a point $\mathbf{r}$, owing to idealized oscillating electric ($\mathbf{p}$) and magnetic ($\mathbf{m}$) dipole moments, produced by transmitting antennae at point $\mathbf{r}'$

$$\begin{bmatrix} \mathbf{E}(\mathbf{r}) \\ c\mathbf{B}(\mathbf{r}) \end{bmatrix} = -H(\mathbf{k}, \mathbf{r}-\mathbf{r}') \begin{bmatrix} c\,\mathbf{p} \\ \mathbf{m} \end{bmatrix} \tag{1}$$

where in free space and in the far-field, H is given by a compact version of the standard formulas that describe the fields radiated by oscillating electric and magnetic dipoles[2] (in SI units):

$$H_0(\mathbf{k}, \mathbf{r}) = \frac{|\mathbf{k}|^3}{\epsilon_0 c} \frac{e^{i\mathbf{k}\cdot\mathbf{r}}}{4\pi\mathbf{k}\cdot\mathbf{r}} \begin{bmatrix} J^2(\hat{\mathbf{r}}) & J(\hat{\mathbf{r}}) \\ -J(\hat{\mathbf{r}}) & J^2(\hat{\mathbf{r}}) \end{bmatrix} \tag{2}$$

Here $\mathbf{k}$ is the wave vector ($|\mathbf{k}| = \omega/c = 2\pi/\lambda$) and $1/\epsilon_0 c \approx 377\,\Omega$ is the impedance of free space (c is the speed of light). $J(\hat{\mathbf{r}})$ is a 3×3 matrix given by $J_{ij}(\hat{\mathbf{r}}) = \Sigma_k \epsilon_{ikj} \hat{\mathbf{r}}_k$, defined so that $J(\hat{\mathbf{r}})\mathbf{p} = \hat{\mathbf{r}} \times \mathbf{p}$ (with $\hat{\mathbf{r}} = \mathbf{r}/|\mathbf{r}|$).

The communication channel associated with equation (1) includes additive noise measured by the receiver. For simplicity, we make the canonical assumption that its components are uncorrelated gaussian white noise with equal variance, and that communication takes place over a sufficiently narrow bandwidth that H has negligible frequency dependence ('flat fading'). For a time-independent H, the rate at which information can be transferred

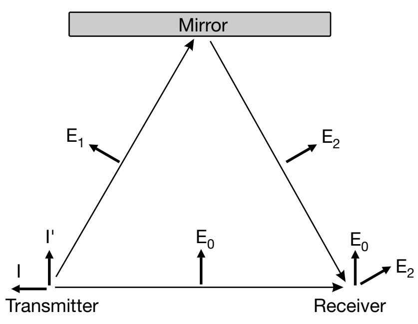

Figure 1 Communicating with electric fields in the presence of a mirror. In the two-dimensional plane of the figure, orthogonal current dipoles at the transmitter, I and I' (left), control two degrees of electric field freedom at the receiver, E_0 and E_2 (right). The direction perpendicular to the plane contributes a third degree of freedom (E_0, E_1, and E_2 are transverse fields on the three paths shown). Normally, due to transverse propagation of electromagnetic waves, there would be no longitudinal electric field component at the receiver. Thus, as is drawn, without the mirror the current dipole labelled I would not produce electric fields at the receiver. However, the alternative propagation path shown causes the component E_2 to appear at the receiver, which has non-zero longitudinal projection when referred to the non-reflected path.

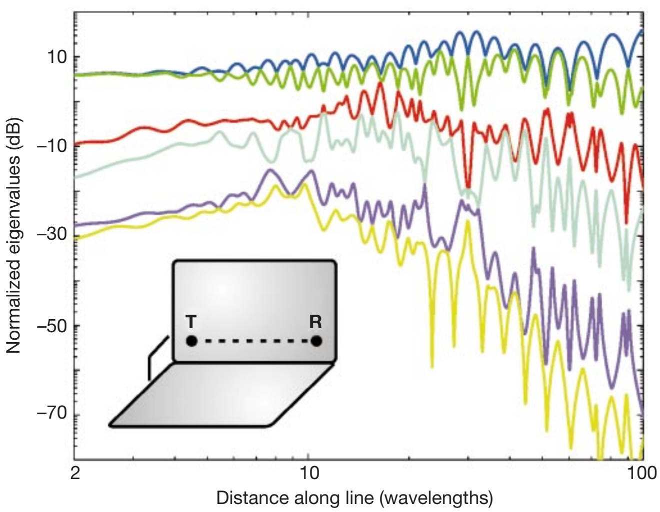

Figure 2 Eigenvalues of $HH^\dagger$ in a two-mirror idealized scattering environment. Data were obtained by simulating the receiver (R) at a variable distance from the transmitter (T) along the line indicated by the inset. The line joins the points $(x, y, z) \approx (9.9, 7.7, 10.5)\lambda$ and $(15.1, 109.8, 8.1)\lambda$, while the mirrors are in the planes $x = 0$ and $z = 0$. Note that rank$(H) = 6$ (that is, there are no eigenvalues equal to zero), indicating a threefold capacity increase over what is possible in free space with no scattering. Eigenvalues are normalized to those that would be obtained in free space: $(|\mathbf{k}|^2/4\pi\epsilon_0|\mathbf{r}|c)^2$. (At large distances the reflections are glancing, which leads to widely spaced eigenvalues). See equations (1) and (2).

between an n-antennae transmitter/receiver pair ($n = 6$ in equations (1) and (2) above) is characterized by the quantity

$$M(H) = \log_2 \det[I + (\rho/n)HH^\dagger] \qquad (3)$$

where $M(H)$, in bits per second per hertz, is the mutual information between the transmitter and receiver when the transmitted signals are uncorrelated white gaussian stochastic processes with equal power. We use units such that the noise components have unit variance, allowing us to denote both total power and signal-to-noise ratio by the same symbol ρ. The significance of $M(H)$ is that for a fluctuating H, under appropriate conditions, the capacity C of the channel is given by the expectation of $M(H)$ taken over the probability distribution of H. The conditions are that H is known by the receiver but not by the transmitter (as would be the case if transmitted pilot signals help the receiver calculate H). We note that if the channel is known to the transmitter, the capacity will be higher and is given by the "water filling" solution where power is unevenly divided among transmitting antennae[6]. Fluctuations in H may be caused by a fluctuating environment or by movement of the antennae.

Clearly, the capacity depends on the rank of H. It follows by inspection that at large signal-to-noise ratio ρ, $M(H)$ (and therefore C) tends to the value $m \log_2 \rho$, where $m = \mathrm{rank}(H)$. We note that the large ρ limit is taken for fixed H. It is easy to verify that the rank of H_0 (see equation (2)) is two, which corresponds to our intuitive notion of there being only two polarization degrees of freedom in free space. We now formally define the number of polarization channels as rank(H). Our basic observation here may be summarized by the statement that it is possible to have rank(H) = 6 in an environment with scattering, with a concomitant increase in the capacity of the wireless communication channel. We note that six independent signals have to be transmitted in order to take advantage of this increased capacity.

A simple geometry which shows that we would expect rank(H) = 6 in scattering environments consists of two perfectly conducting planes (mirrors) at right angles to each other (inset of Fig. 2). The matrix H (equation (1)) in this environment may be computed by summing over free-space contributions like H_0 (equation (2)) corresponding to the actual transmitter and its images in the two mirrors (two single and one double reflection). We plot the eigenvalues of $HH^\dagger$ for the transmitter and receiver placed along a given line in the simulated environment (Fig. 2); we note that all six eigenvalues are non-zero and hence rank(H) = 6, signifying a threefold increase in capacity over what would be possible in free space. An alternative way of seeing that all six components of the electromagnetic field can fluctuate independently is to consider their covariance at a point due to an isotropic distribution of plane waves. It is easy to verify in this case that all off-diagonal covariances vanish, so that no vector component can be predicted from any other.

Apart from increasing the number of degrees of freedom in wireless electromagnetic communications, the existence of six independent channels as indicated by the full rank of H also implies improved fading performance of a receiver sensitive to polarization degrees of freedom. As the environment fluctuates, or as the receiver moves through space, the measured electric and magnetic fields also fluctuate. For an antenna sensitive to just a single field component the amplitude can occasionally come close to zero (fading); however, it is quite unlikely that all six vector components will vanish simultaneously. Thus, by taking full advantage of the receive diversity that is offered by polarization (which we noted is already done for two polarization states[3]) the fading can be greatly ameliorated. In contrast with earlier proposals[4–7], where scattering leads to greater spatial diversity, the subject of this Letter involves measurements theoretically localizable at only one spatial point, thus leading to more compact antenna designs for similar capacity gains. At one spatial point it is possible to measure two three-dimensional vector fields (electric and magnetic); we do not consider, however, measurements of spatial field derivatives, which are independent degrees of freedom and in principle could lead to further increases in capacity beyond the factor of three considered here. Completely variable vector electric and magnetic fields seem only to have been discussed previously in direction-finding applications[9–11].

Our experimental work demonstrates the increase in capacity originating from the three electric polarization states in a scattering environment. Dubbed a "tripole", the antenna system consists of three standard sleeves[12] arranged orthogonally as shown in Fig. 3. Each antenna element is roughly a half wavelength long (~17 cm), and was trimmed for efficient resonant operation at 880 MHz by adjusting variable length sections. Each has good coupling of power to radiated modes with less than 5% power reflected back to the transmitting source. As the three elements are orthogonal and cross close to their feed points, coupling among them is minimized (less than −25 dB of power) and we find the radiation pattern of each element in the tripole to be similar to that of an isolated sleeve including deep nodes (−25 dB of power) along the axes. The three antennae together can create an arbitrary vector electric dipole

Figure 3 Tri-polarized antenna (tripole). The composite structure is composed of three orthogonal sleeves[12] with their feed points collocated at the centre of the image. Each has two variable length segments which are adjusted to efficiently couple radiation to its transmission line. The three antennae together can create an arbitrary vector electric dipole moment at the transmitter, as well as function as detectors of the vector electric field at the receiver.

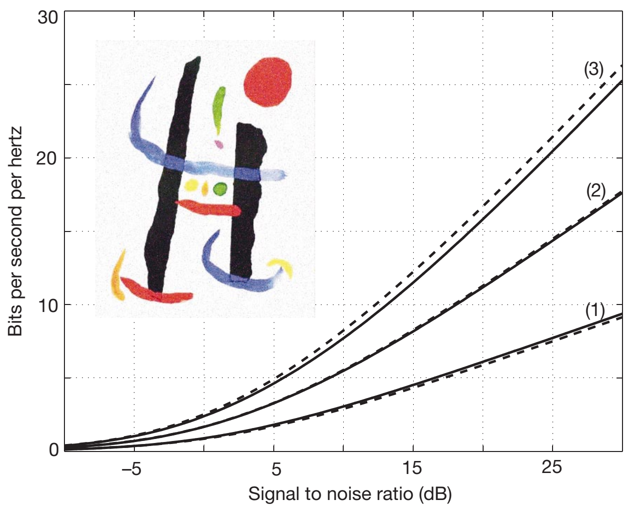

Figure 4 Capacity of the tripole antenna. Shown are experimentally obtained capacity estimates for one (lower solid line), two and three (upper solid lines) orthogonal sleeve antennae (Fig. 3), calculated from measured transfer matrices H. Dotted lines are from the random matrix-based theory[6]. Inset, here we show a capacity increase through the transfer of actual data. The reconstructed colour image above (Joan Miro, *A toute épreuve*) was transmitted as three distinct red, green, and blue monochrome subfields on each of the three orthogonally oriented antennae of Fig. 3 (that is, red was transmitted on $\hat{\mathbf{x}}$ polarization, green on $\hat{\mathbf{y}}$, and blue on $\hat{\mathbf{z}}$).

moment at the transmitter, as well as function as detectors of the vector electric field at the receiver. As for the magnetic polarization components, we assume that three more resonant antenna structures, perhaps mutually orthogonal magnetic-sensing 'loops', could be designed to be collocated with the three orthogonal (electric-sensing) sleeves. Although the engineering details associated with magnetic-sensing antennae differ from those of electric-sensing ones, these differences have been successfully dealt with before[12,13].

Having constructed two such tri-polarized antennae, demonstrating their potential for increased capacity in a particular environment involves measuring the rank of the 3×3 electric transfer matrix H (that is, equation (1)) where contributions from **B** and **m** are ignored). A variety of pilot signals may be used to measure the transfer matrix H, but we chose simple sinusoids (tones) for purposes of characterization. Let α and β each denote one of the three indices of the transmit and receive antennae polarizations. The experimental procedure was to choose three distinct tones ω_β within a narrow frequency band (experimentally, it is found that H (equation (1)) varies negligibly over bands of 20 kHz) and transmit each on its own antenna element. All three frequencies were then observed on each of the three antenna elements at the receiver. The transfer matrix element $H_{\alpha\beta}$ could then be read off as the complex amplitude at frequency ω_β (transmitted on antenna β) received on antenna α.

The results are illustrated in the graph of Fig. 4, and show capacities inferred from the measured matrices. The upper curve is the "tripole" capacity (3×3 matrix), whereas the lower and middle curves are for 1×1 (scalar) and 2×2 (dual-polarized) submatrices, respectively. In the scalar and dual-polarized cases we present capacities averaged over the nine possible choices for antennae at the transmitter and receiver. (There are three possible ways of choosing either one or two antennae from three, and combinations of transmit and receive elements yields 3×3 or nine possibilities.) It is clear from the figure that use of polarization adds to the capacity, and does so in agreement with theory[6]. These data were taken in a large cafeteria (about 500 m^2, with 10-m high ceilings) with the transmitter and receiver around a corner from one another; each matrix was measured with the receiver at a different position but always about 25 m from the transmitter.

In order to provide an illustrative visual example of the expansion of channel capacity, we wirelessly communicated a colour image with colour represented as usual by a three-dimensional vector of red, green and blue components. These three monochrome image components of the original full-colour image were transmitted separately by each of the three transmit antennae, along with pilot signals allowing for measurement of the 3×3 transfer matrix H. The inset of Fig. 4 shows the recovered image (Joan Miro, *A toute épreuve*).

From these studies it is clear that electromagnetic polarization can play an important role in wireless communication. We have demonstrated experimentally the capacity increase that comes from exploiting the three-dimensional electric field vector (Fig. 4), and have theoretically shown the benefit arising from the use of magnetic degrees of freedom as well (Fig. 2). There will undoubtedly be practical issues to be considered in using a sixfold polarized antennae system, including the efficiency and cross-coupling of antennae extracting all the electromagnetic degrees of freedom near a point, as well as issues such as the statistics and environmental fluctuations that affect H. Nevertheless, the capacity increase is real and necessitates a re-evaluation of the use of polarization in wireless communication using electromagnetic waves. □

Received 4 July; accepted 26 October 2000.

1. Andrews, E. L. $50 billion for German wireless licenses. *The New York Times* 18 August (2000).
2. Jackson, J. D. *Classical Electrodynamics* (John Wiley, New York, 1975).
3. Singer, A. Space vs. polarization diversity. *Wireless Rev.* **15,** 164–166 (1998).
4. Winters, J. H. On the capacity of radio communication systems with diversity in a rayleigh fading environment. *IEEE J. Selected Areas Commun.* Vol. SAC-5, 871–878 (1987).
5. Foschini, G. J. & Gans, M. J. On limits of wireless communications in a fading environment when using multiple antennas. *Wireless Pers. Commun.* **6,** 311–335 (1998).
6. Telatar, I. E. Capacity of multi-antenna gaussian channels. *Eur. Trans. Telecommun.* **10,** 585–595 (1999).
7. Moustakas, A. L., Baranger, H. U., Balents, L., Sengupta, A. M. & Simon, S. Communication through a diffusive medium: Coherence and capacity. *Science* **287,** 287–290 (2000).
8. deCarvalho, R., Mitra, P. P. & Andrews, M. R. in *National Radio Science Meeting* 84 (International Union of Radio Science, National Academy of Sciences, 2000).
9. Morgan, M. & Evans, W. Synthesis and analysis of elliptic polarization loci in terms of space-quadrature sinusoidal components. *Proc. IRE* **39,** 552–556 (1951).
10. Hatke, G. F. in *Twenty-seventh Asilomar Conference on Signals, Systems & Computers* 1365–1369 (IEEE Computer Society Press, Los Alamitos, California, 1993).
11. Afraimovich, E. L., Chernukhov, V. V., Kobzar, V. A. & Palamartchouk, K. S. Determining polarization parameters and angles of arrival of hf radio signals using three mutually orthogonal antennas. *Radio Sci.* **34,** 1217–1225 (1999).
12. Kraus, J. D. *Antennas* 2nd edn 725–726 (McGraw Hill, Boston, 1988).
13. Lee, W. C. Y. Theoretical and experimental study of the properties of the signal from an energy-density mobile-radio antenna. *IEEE Trans.* **1,** 25–32 (1967).

Acknowledgements

This work is supported by internal funding at Bell Labs, Lucent Technologies. We are grateful to W. M. MacDonald for his assistance in characterizing our antenna's radiation patterns, and to M. J. Gans for his insights and discussions concerning magnetic polarization.

Correspondence and requests for materials should be addressed to M.R.A. (e-mail: mikea@bell-labs.com).

Relationship between structural order and the anomalies of liquid water

Jeffrey R. Errington & Pablo G. Debenedetti

Department of Chemical Engineering, Princeton University, Princeton, New Jersey 08544-5263, USA

In contrast to crystalline solids—for which a precise framework exists for describing structure[1]—quantifying structural order in liquids and glasses has proved more difficult because even though such systems possess short-range order, they lack long-range crystalline order. Some progress has been made using model systems of hard spheres[2,3], but it remains difficult to describe accurately liquids such as water, where directional attractions (hydrogen bonds) combine with short-range repulsions to

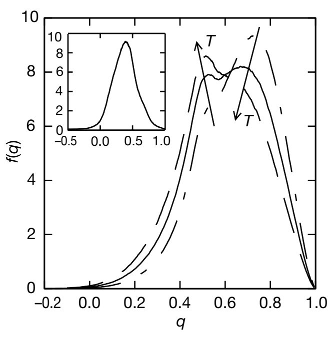

Figure 1 The effect of temperature on the distribution of the orientational order, q, at a density $\rho = 1.2\,\mathrm{g\,cm^{-3}}$. Three temperatures T are considered; 320 K (dashed line), 280 K (solid line) and 240 K (dot-dashed line). The fraction of molecules with q-values between $q + \mathrm{d}q/2$ and $q - \mathrm{d}q/2$ is $f(q)\mathrm{d}q$. The area under each curve is normalized to unity. Arrows indicate the effect of increasing temperature. The possible range of q for a molecule is $-3 \le q \le 1$; the average value for a collection of molecules spans the range $0 \le \langle q \rangle \le 1$. Inset, the q-distribution for a Lennard–Jones system at a density $\rho^* = N\sigma^3/V = 1.0$ and temperature $T^* = k_B T/\epsilon = 2.0$, where ϵ and σ are the energy and size parameters, and k_B is Boltzmann's constant. For the Lennard–Jones fluid, $f(q)$ is virtually unchanged throughout the liquid region of the phase diagram.